Regular Article

PHYSICAL CHEMISTRY RESEARCH
Published by the
Iranian Chemical Society
www.physchemres.org
info@physchemres.org

***Phys. Chem. Res.**, Vol. 6, No. 4, 871-878, December 2018*
DOI: 10.22036/pcr.2018.148943.1543

DFT Study of Adsorption of Lithium on Si, Ge-doped Divacancy Defected Graphene as Anode Material of Li-ion Battery

M.M. Loghavi[a,b], H. Mohammadi-Manesh[b,*], R. Eqra[a], A. Ghasemi[a] and M. Babaiee[a]

[a]*Institute of Mechanics, Iranian Space Research Center, Shiraz, Iran*
[b]*Department of Chemistry, Yazd University, Yazd, Iran*

(Received 26 September 2018, Accepted 24 October 2018)

Graphene is an anode material that is expected to be a good alternative for graphite to increase the capacity and rate-capability of lithium-ion batteries. Graphene synthesis is always accompanied by defects in the structure. The most common defect in graphene is the divacancy (DV) defect. In this study, the effect of this defect on the lithium adsorption was studied by density functional theory method. In addition, the doping effect of silicon and germanium atoms on the defective graphene structure was investigated. The bandgap energy of DV-defected graphene, which has an inverse relationship with electrical conductivity, remains constant with addition of germanium and decreases with addition of silicon. In all cases, along with lithium adsorption, the bandgap energy is increased, so that the germanium doped compound has the highest bandgap and the structure with no doped atom has the least bandgap. However, the difference in the minimum and maximum bandgap in structures is very low. The results show that the addition of silicon and germanium leads to stronger adsorption of lithium which means it is possible to raise the charge-discharge capacity of graphene through doping with elements while the material still has a high charge/discharge capability.

Keywords: Adsorption, DFT, Defect, Doped, Graphene, Li-ion battery

INTRODUCTION

Li-ion batteries (LIBs) are the next-generation energy storage devices because of their high-energy content, good cyclability, small self-discharge, no memory effect, high average voltage and wide operating temperature window [1]. Many research activities on lithium-ion batteries focus on the discovery of anode material such as metals, metal oxides, oxysalts and non-metals with high capacity, good cycling and suitable operating voltage [2-6]. The use of graphene and its composites as an anode active material in lithium-ion batteries has been investigated extensively [7-11].

Graphene has a two-dimensional hexagonal structure of carbon atoms that is really the essential structure block for all other sp^2-hybridized carbon arrangements, such as graphite, fullerenes, and carbon nanotubes. It is a remarkable material because of its mechanical, electrical, thermal and optical properties. The notable structure and specific properties of graphene make vast applications in different fields such as sensors, transistors, photovoltaic cell, gas separation membranes and specifically in batteries [12-14]. Theoretical studies have been carried out for better understanding the interaction of lithium with graphene in LIBs. Lee *et al.* performed a comprehensive first-principles investigation of Li absorption and intercalation in single layer and few layer graphene, as compared to bulk graphite. They have predicted that there exists no lithium arrangement that stabilizes Li absorption on the surface of single layer graphene unless that surface contains defects [15]. Chouhan *et al.* studied the lithium adsorption on epoxy

*Corresponding author. E-mail: mohammadimanesh@yazd.ac.ir

and hydroxyl functionalized graphene sheet using DFT and found that these types of graphene provide the highest specific capacity of 860 mAh g^{-1} [16]. Denis considered the interaction of Li with monodoped (X) and dual-doped graphene (XY), X = Al, Si, P and S and Y = B, N and O. He has found that Dual-doped graphene is a good choice to modulate the interaction of Li with graphene [17].

Robertson *et al.* studied the defects in graphene by aberration corrected high resolution transmission electron microscopy (AC-TEM) and it revealed that DV defect is the most abundant defect in the structure of graphene [18]. The DV-defected graphene is the result of rebuilding two bonds after leaving a pair of atoms, leading to a 5-, 8-, 5-membered ring arrangement, often categorized as a (5-8-5) vacancy, as shown in Fig. 1.

To the best of our knowledge, the effect of this defect on the adsorption of lithium by graphene has not been studied yet. In the present study, DV-defected graphene was modeled in pure state and in doped states with silicon and germanium. Lithium adsorption by these structures was studied *via* density functional theory (DFT) calculations, in order to investigate the possibility of using these materials as an anode material in a Li-ion battery. Energy difference between HOMO and LUMO (bandgap energy), electronic charge distribution and adsorption energy are computed and analyzed.

COMPUTATIONAL METHODS

Adsorption of Li on different graphene sheets was investigated by DFT calculations using the SIESTA code [19]. In this study, DV-defected graphene ($C_{30}H_{14}$), Si-doped DV-defected graphene ($C_{29}H_{14}Si$), Ge-doped DV-defected graphene ($C_{29}H_{14}Ge$) and lithium were used as the parent samples. There are four possible sites for adsorption of Li on target atom (T atom; C or Si or Ge) of graphene sheet: the bridge sites at the middle of T-C bonds, the top site straight above a T atom and the hollow site at the center of an octagon (see Fig. 2). The generalized gradient approximation (GGA) of Perdew-Burke-Ernzerhof (PBE) [20] with double-zeta polarization (DZP) basis set were used in simulations. Initially, each of the graphene structure was optimized individually in the presence and absence of lithium. No symmetry constraints were considered for geometry optimizations. Then, the energy of the systems was calculated in their equilibrium state.

RESULTS AND DISCUSSION

There are two non-equivalent sites for the dopant (Si or Ge) atoms. One site, shown in Fig. 2, lies at the intersection of pentagonal and hexagonal carbon rings, while the site exists at the intersection of two hexagonal carbon rings. We selected the location between the two 5- and 6-member rings to create the maximum structural defect in the structure, and the possibility of lithium adsorption was investigated in these cases. In fact, we did not seek to find the proper location of doping in this study; just wanted to investigate the amount of energy changes in lithium adsorption by adding germanium and silicon elements in a definite location from a thermodynamically stable structure.

The distribution of HOMO-LUMO orbitals on atoms constituting a structure has a great influence on the absorption properties of a material. Figure 3 shows that the HOMO orbitals are on all carbons of DV-defected graphene, but with the introduction of silicon and germanium to the structure, these two atoms have a larger share of orbitals than carbon atoms. By examining the LUMO orbitals, it is observed that the DV defect in the structure has led to the major focus of the LUMO orbitals on the 5- and 8-membered rings. Both the entry of the doping element and the presence of the defect indicate their active participation in conduction process.

Figure 4 illustrates electronic charge distribution on the optimized graphene structures. It is clear that in the DV-defected graphene, the positive charge distribution is almost symmetric around the carbon atoms, but in the Si- and Ge-doped DV-defected graphene structures, positive charge distribution is deformed in the vicinity of doped atoms. Based on these images, it is well understood that graphene is re-arranged to create a negative charge around the doped atom and facilitates Li adsorption.

The adsorption energy (in eV) of Li on graphene samples is defined as:

$$E_{ad} = (E_{gr} + E_{Li}) - E_{gr\text{-}Li} \quad (1)$$

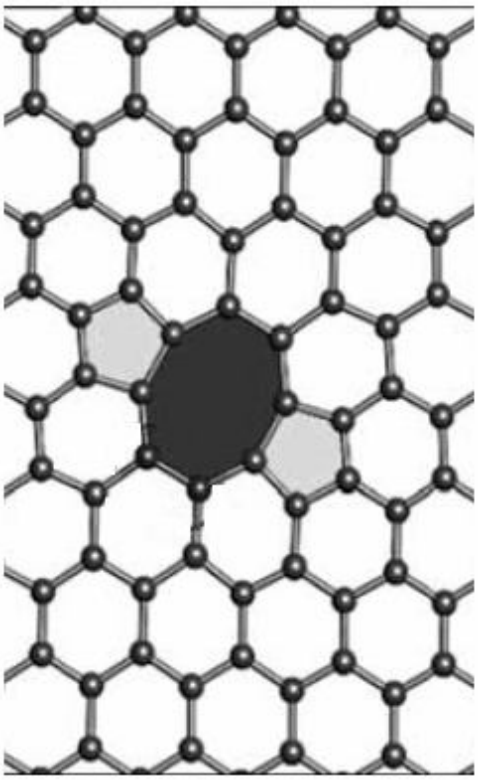

Fig. 1. Atomistic model of a (5-8-5) DV-defected graphene [18].

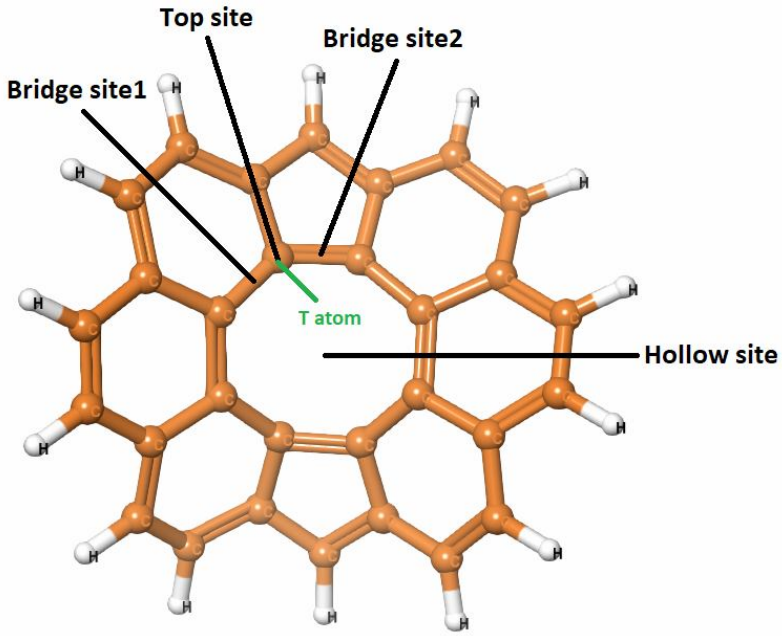

Fig. 2. Four different adsorption sites of Li atom relative to the C, Si, or Ge atomic location.

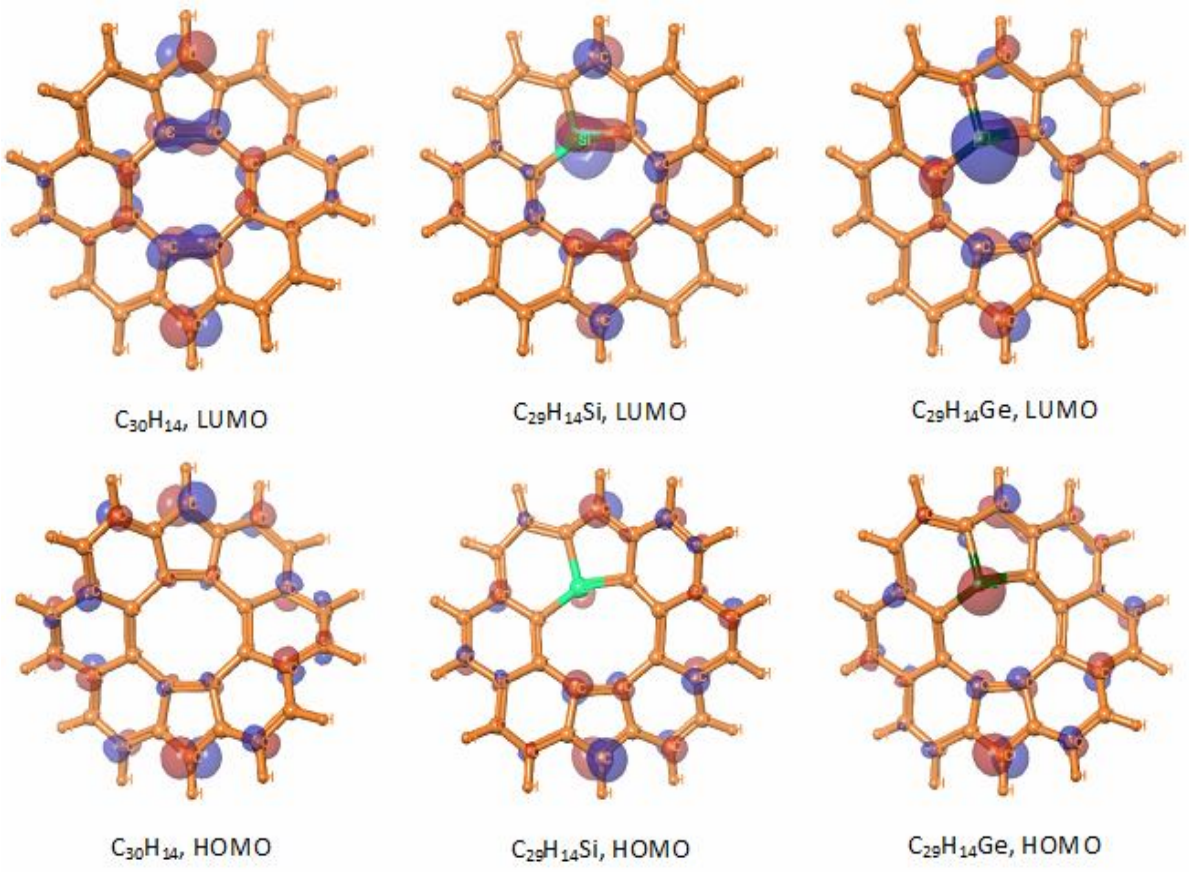

Fig. 3. The HOMO, LUMO orbitals for different structures of graphene (isosurface value = 0.03 a.u.).

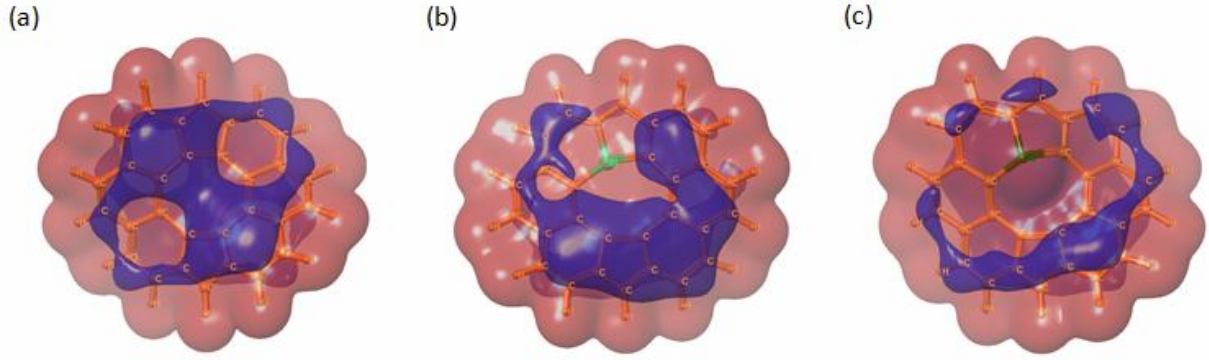

Fig. 4. Electronic charge distribution for: (a) $C_{30}H_{14}$, (b) $C_{29}H_{14}Si$ and (c) $C_{29}H_{14}Ge$ (red: negative charge, blue: positive charge).

where, $E_{gr\text{-}Li}$, E_{gr} and E_{Li} are the total energies of the graphene/Li structures, isolated graphene sheets ($C_{30}H_{14}$, $C_{29}H_{14}Si$ or $C_{29}H_{14}Ge$) and isolated Li, respectively. Here, a positive E_{ad} represents an attractive interaction between graphene and Li, while a negative E_{ad} corresponds to the adsorbed structures which are thermodynamically unstable

Table 1. Lithium Adsorption Energies (in eV) on Different Graphene Sheets

Sample	Hollow site	Top site	Bridge site1	Bridge site2
DV-defected graphene	1.576	1.576	1.575	1.575
Si-doped DV-defected graphene	1.846	2.021	2.023	1.670
Ge-doped DV-defected graphene	1.983	2.195	2.198	2.196

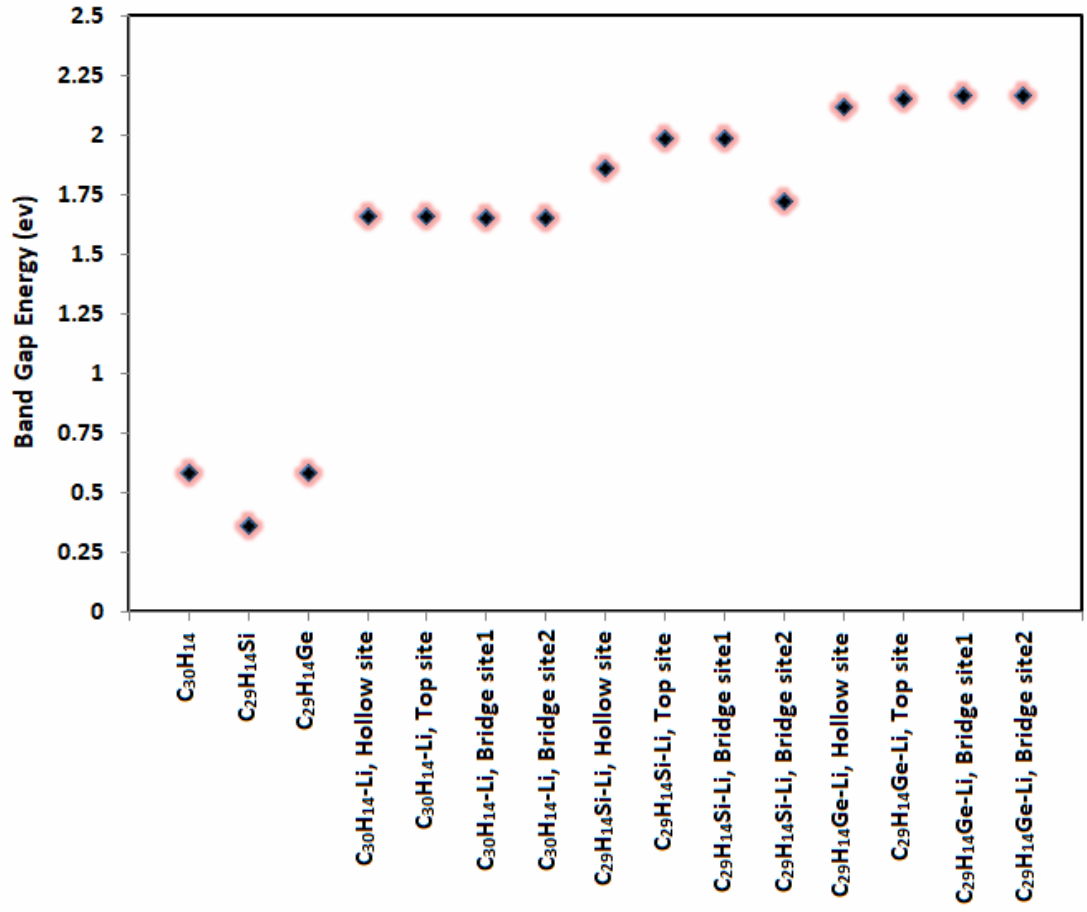

Fig. 5. The bandgap energy of different graphene sheets with and without adsorbed lithium.

relative to the host graphene structures and separated Li atom [21,22]. The values of lithium adsorption energy in various graphene structures are presented in Table 1. As can be seen, in all cases, the adsorption energy has a positive value, indicating the tendency of graphene-based structures for Li adsorption. The amount of energy released from the lithium adsorption process at different sites of DV-defected graphene is not much different. By the addition of silicon and germanium to DV-defected graphene, adsorption is more facilitated. The greatest amount of adsorption energy

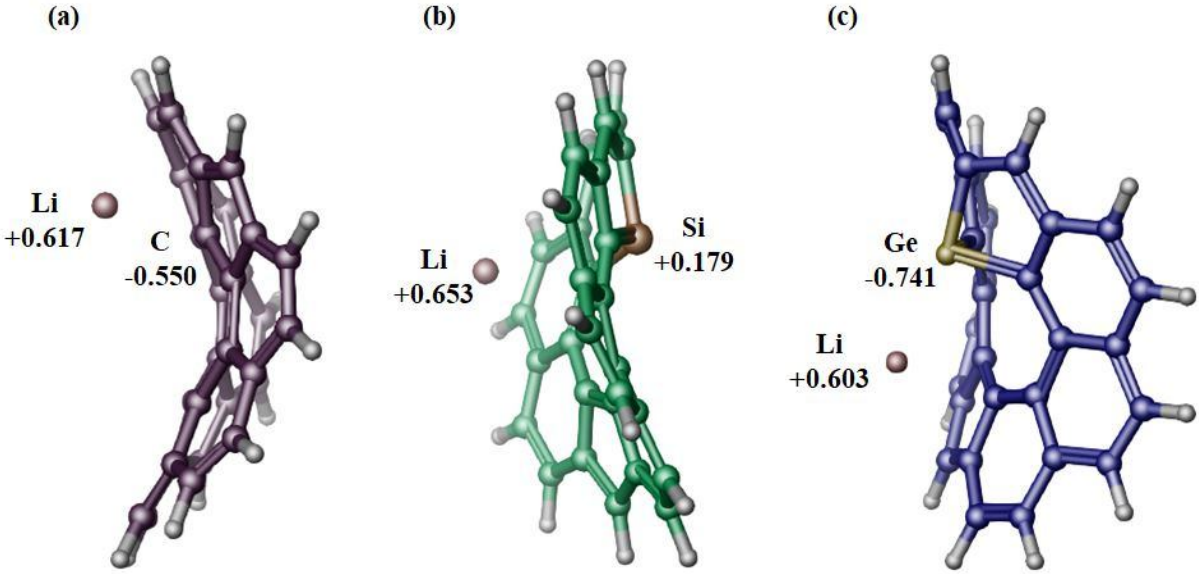

Fig. 6. Side view of the orientation of graphene atoms against lithium: (a) $C_{30}H_{14}Li$ (Top site), (b) $C_{29}H_{14}Si$ (Bridge site1) and (c) $C_{29}H_{14}Ge$ (Bridge site1).

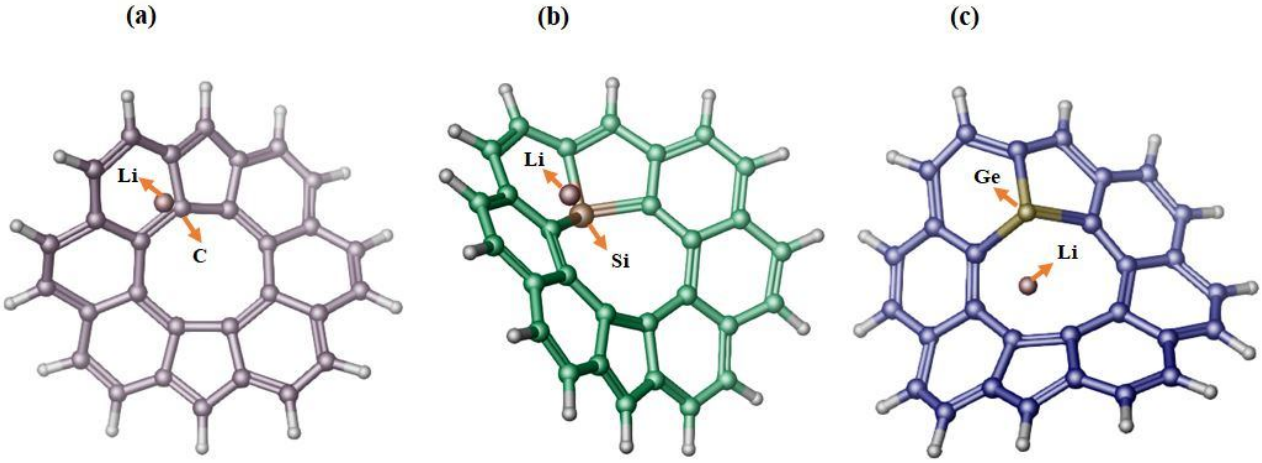

Fig. 7. Top view of the orientation of graphene atoms against lithium: (a) $C_{30}H_{14}Li$ (Top site), (b) $C_{29}H_{14}Si$ (Bridge site1) and (c) $C_{29}H_{14}Ge$ (Bridge site1).

belongs to the structures doped with Ge atom.

What is certain is that by increasing the size of graphene, different configurations can be created, and there are more non-equivalent points that can have different adsorption energies. However, here, a structure with the same number of atoms and atomic positions is considered for all cases allowing us to compare the effect of doping in them. In future work, we can examine the effect of graphene size and other doping sites on adsorption.

Figure 5 shows the bandgap energy of graphene structures before and after adsorption of lithium. All three grapheme parent materials have low bandgap, indicating

their conducting nature. Among them, Si-doped DV-defected graphene ($C_{29}H_{14}Si$) is found to have the lowest bandgap (0.36 eV) with the HOMO/LUMO levels coming closer to each other. This shows that graphene bandgap is adjustable through doping. By adsorbing lithium, bandgap of parent structures becomes more open. The order of bandgap increases as follows: Ge-doped DV-defected graphene > Si-doped DV-defected graphene > DV-defected graphene. Comparing the results of adsorption energy and bandgap shows that lithium adsorption is less likely to occur on a site that produces less bandgap. $C_{29}H_{14}$Si-Li-Bridge-site2 and $C_{29}H_{14}$Ge-Li-Hollow-site are two obvious examples of this case.

Figures 6 and 7 show how the atoms of graphene structures are oriented toward lithium. For each structure, the most stable mode is displayed and partial charges of T atom and Li are presented. As can be seen, DV-defected graphene atoms are oriented symmetrically toward lithium. However, silicon and germanium atoms in Si- and Ge-doped DV-defected graphene structures, with respect to their partial charge, have been displaced in such a way that lithium is adsorbed more strongly compared to DV-defected graphene.

CONCLUSIONS

In this research, graphene containing DV defect was modeled and germanium and silicon atoms were added to the structure, separately. The DFT calculations demonstrate that the adsorption of Li on the surface of the doped and undoped structures is exothermic and thermodynamically favorable. Comparison of the results indicate that the adsorption energy of the Si- and Ge-doped structures is more than undoped structure. The HOMO-LUMO results reveal that Si and Ge atoms have a larger share of LUMO orbitals than that of carbon atoms. On the other hand, the DV defect in the structure has led to the main localization of the LUMOs density on the 5- and 8-membered rings. Therefore, both the DV defect and the doping play an important role in the electrical properties of graphene and the adsorption of lithium.

In summary, if the synthesized graphene containing DV defect is doped with silicon and germanium atoms, it can be used as a high-lithium acceptance anode material in lithium ion batteries with the ability of high-rate charge and discharge.

REFERENCES

[1] Wang, H.; Li, X.; Baker-Fales, M.; Amama, P. B., 3D graphene-based anode materials for Li-ion batteries. *Curr. Opin. Chem. Eng.* **2016**, *13*, 124-132, DOI: 10.1016/j.coche.2016.08.009.

[2] Reddy, M.; Subba Rao, G.; Chowdari, B., Metal oxides and oxysalts as anode materials for Li ion batteries. *Chem. Rev.* **2013**, *113*, 5364-5457, DOI: 10.1021/cr3001884.

[3] Liu, J.; Kopold, P.; van Aken, P. A.; Maier, J.; Yu, Y., Energy storage materials from nature through nanotechnology: A sustainable route from reed plants to a silicon anode for lithium-ion batteries. *Angewandte Chemie.* **2015**, *127*, 9768-9772, DOI:

[4] Wang, S.; Wang, R.; Chang, J.; Hu, N.; Xu, C., Self-supporting Co_3O_4/graphene hybrid films as binder-free anode materials for lithium ion batteries. *Scientific Reports.* **2018**, *8*, 3182, DOI:

[5] Lin, X.; Zhang, J.; Tong, X.; Li, H., Pan, X.; Ning, P.; Li, Q., Templating synthesis of Fe_2O_3 hollow spheres modified with Ag nanoparticles as superior anode for lithium ion batteries. *Scientific reports.* **2017**, *7*, 9657, DOI:

[6] Yi, T. -F.; Zhu, Y. -R.; Tao, W.; Luo, S.; Xie, Y.; Li, X. -F., Recent advances in the research of $MLi_2Ti_6O_{14}$ (M = 2Na, Sr, Ba, Pb) anode materials for Li-ion batteries. *J. Power Sources.* **2018**, *399*, 26-41, DOI:

[7] Wang, H.; Cui, L. -F.; Yang, Y.; Sanchez Casalongue, H.; Robinson, J. T., Liang, Y.; Cui, Y.; Dai, H., Mn_3O_4- graphene hybrid as a high-capacity anode material for lithium ion batteries. *JACS.* **2010**, *132*, 13978-13980, DOI: 10.1021/ja105296a.

[8] Liu, J. -Y.; Li, X. -X.; Huang, J. -R.; Li, J. -J.; Zhou, P.; Liu, J. -H.; Huang, X. -J., Three-dimensional graphene-based nanocomposites for high energy density Li-ion batteries. *J. Mater. Chem.* **2017**, *5*, 5977-5994, DOI: 10.1039/C7TA00448F.

[9] Qi, W.; Li, X.; Li, H.; Wu, W.; Li, P.; Wu, Y.; Kuang, C.; Zhou, S.; Li, X., Sandwich-structured nanocomposites of N-doped grapheme and nearly

monodisperse Fe_3O_4 nanoparticles as high-performance Li-ion battery anodes. *Nano Res.* **2017**, *10*, 2923-2933, DOI: 10.1007/s12274-017-1502-x.

[10] Puttapati, S. K.; Gedela, V.; Srikanth, V. V.; Reddy, M.; Adams, S.; Chowdari, B., Unique reduced graphene oxide as efficient anode material in Li ion battery. *Bull. Mater. Sci.* **2018**, *41*, 53, DOI: 10.1007/s12034-018-1575-5.

[11] Shi, W.; Zhang, Y.; Key, J.; Shen, P. K., Three-dimensional graphene sheets with NiO nanobelt outgrowths for enhanced capacity and long term high rate cycling Li-ion battery anode material. *J. Power Sources*. **2018**, *379*, 362-370, DOI: 10.1016/j.jpowsour.2018.01.025.

[12] Kimiagar, S.; Rajabpour, A.; Tavazoee, F., Effect of defects on mechanical properties of graphene under shear loading using molecular dynamic simulation. *Phys. Chem. Res.* **2015**, *3*, 299-304, DOI: 10.22036/PCR.2015.10716.

[13] Dhakate, S.; Chauhan, N.; Sharma, S.; Tawale, J.; Singh, S.; Sahare, P.; Mathur, R., An approach to produce single and double layer graphene from re-exfoliation of expanded graphite. *Carbon*. **2011**, *49*, 1946-1954, DOI: 10.1016/j.carbon.2010.12.068.

[14] Shokuhi Rad, A., DFT study of nitrous oxide adsorption on the surface of Pt-decorated graphene. *Phys. Chem. Res.* **2016**, *4*, 619-626, DOI: 10.22036/PCR.2016.16428.

[15] Lee, E.; Persson, K. A., Li absorption and intercalation in single layer graphene and few layer graphene by first principles. *Nano Lett.* **2012**, *12*, 4624-4628, DOI: 10.1021/nl3019164.

[16] Chouhan, R. K.; Raghani, P., Enhanced Li capacity in functionalized graphene: A first principle study with van der Waals correction. *J. Appl. Phys.* **2015**, *118*, 125101, DOI: 10.1063/1.4931152.

[17] Denis, P. A., Lithium adsorption on heteroatom mono and dual doped graphene. *Chem. Phys. Lett.* **2017**, *672*, 70-79, DOI: 10.1016/j.cplett.2017.01.036.

[18] Robertson, A. W.; Warner, J. H., Atomic resolution imaging of graphene by transmission electron microscopy. *Nanoscale*. **2013**, *5*, 4079-4093, DOI: 10.1039/c3nr00934c.

[19] Soler, J. M.; Artacho, E.; Gale, J. D.; García, A.; Junquera, J.; Ordejón, P.; Sánchez-Portal, D., The SIESTA method for *ab initio* order-N materials simulation. *J. Phys.: Condens. Matter*. **2002**, 14, 2745, DOI: 10.1088/0953-8984/14/11/302.

[20] Perdew, J. P.; Burke, K.; Ernzerhof, M., Generalized gradient approximation made simple. *Phys. Rev. Lett.* **1996**, 77, 3865, DOI: 10.1103/PhysRevLett.77.3865.

[21] Kulish, V. V.; Ng, M. -F.; Malyi, O. I.; Wu, P.; Chen, Z., Improved binding and stability in Si/CNT hybrid nanostructures via interfacial functionalization: a first-principles study. *RSC Adv.* **2013**, 3, 8446-8453, DOI: 10.1039/C3RA40340H.

[22] Geng, W.; Liu, H.; Yao, X., Enhanced photocatalytic properties of titania-graphene nanocomposites: a density functional theory study. *Phys. Chem. Chem. Phys.* **2013**, 15, 6025-6033, DOI: 10.1039/c3cp43720e.